·论著·

多参数磁共振成像联合LI-RADS分级标准对肝硬化再生结节与小肝癌的诊断价值及临床意义

蔡宁,石惠,李真真,郭君武
(郑州大学第二附属医院医学影像学科,郑州 450003)

摘要 目的 探讨多参数磁共振成像(Mp-MRI)联合肝脏影像报告和数据管理系统(LI-RADS)分级标准对肝硬化再生结节与小肝癌(SHCC)的诊断价值及临床意义。**方法** 选取2019年3月至2023年3月我院直径≤3 cm的肝脏结节患者86例(132个结节),根据手术病理结果将肝硬化再生结节38例(54个结节)记为良性组,SHCC 48例(78个结节)记为恶性组。比较2组LI-RADS分级和Mp-MRI参数[增强率(ER)、平均强化时间(MET)、最大上升斜率(MSI)、最大下降斜率(MSD)、表观扩散系数(ADC)、脂肪分数(FF)],分析其诊断价值。**结果** 经LI-RADS分级标准诊断,132个结节中共检出阳性76个,阴性56个,其中假阳性10个,假阴性12个;恶性组ER、MET、MSI、ADC低于良性组,FF、MSD高于良性组($P < 0.05$);受试者操作特征(ROC)曲线分析结果显示,Mp-MRI参数联合LI-RADS分级标准诊断肝硬化再生结节与SHCC的曲线下面积(AUC)为0.946(95%*CI*:0.892~0.977),约登指数为0.811,灵敏度为88.46%,特异度为92.59%,优于各Mp-MRI参数及LI-RADS分级单独诊断;恶性组不同病理分级结节LI-RADS分级比较,差异有统计学意义($P < 0.05$);ER、MET、MSI、ADC在高分化结节中最高,中分化结节次之,低分化结节最低,FF、MSD在低分化结节最高,中分化结节次之,高分化结节最低($P < 0.05$);Spearman相关性分析结果显示,LI-RADS分级、ER、MET、MSI、ADC与SHCC病理分级呈正相关,FF、MSD与SHCC病理分级呈负相关($P < 0.05$)。**结论** Mp-MRI参数联合LI-RADS分级标准诊断肝硬化再生结节与SHCC的价值可靠,且能为临床评估SHCC病理分级提供参考依据。

关键词 肝硬化再生结节;小肝癌;多参数磁共振成像;肝脏影像报告和数据管理系统分级标准;诊断价值
中图分类号 R445.2 **文献标志码** A **文章编号** 0258-4646(2024)08-0686-06
网络出版地址 https://link.cnki.net/urlid/21.1227.R.20240722.1245.016
DOI:10.12007/j.issn.0258-4646.2024.08.003

Diagnostic value and clinical significance of Mp-MRI combined with the LI-RADS grading criteria for regenerated nodules in cirrhosis and small heptocellular carcinoma

CAI Ning, SHI Hui, LI Zhenzhen, GUO Junwu
(Medical Imaging Department, The Second Affiliated Hospital of Zhengzhou University, Zhengzhou 450003, China)

Abstract Objective To explore the diagnostic value and clinical significance of multi-parametric magnetic resonance imaging (Mp-MRI) combined with the liver imaging reporting and data system (LI-RADS) grading criteria for diagnosing regenerative nodules and small hepatocellular carcinoma (SHCC) in patients with cirrhosis. **Methods** Eighty-six patients (132 nodules) admitted to our hospital from March 2019 to March 2023 with liver nodules of ≤3 cm in diameter were selected. Based on the surgical pathology results, 38 cases (54 nodules) of regenerative nodules in liver cirrhosis were classified into the benign group, and 48 cases (78 nodules) of SHCC were classified into the malignant group. LI-RADS classification and Mp-MRI parameters [enhancement rate (ER), mean enhancement time (MET), maximum slope of increase (MSI), maximum slope of decrease (MSD), apparent diffusion coefficient (ADC), and fat fraction (FF)] were compared between the two groups, and their diagnostic values were analyzed. **Results** Based on the LI-RADS classification standard, 76 positive and 56 negative nodules were detected among the 132 nodules, including ten false positives and 12 false negatives. The ER, MET, MSI, and ADC were lower in the malignant group than in the benign group, whereas the FF and MSD were higher in the malignant group than in the benign group ($P < 0.05$). The area under the receiver operating characteristic (ROC) curve for the combined diagnosis of liver cirrhosis regenerative nodules and SHCC using Mp-MRI parameters and the LI-RADS classification standard was 0.946 (95%*CI*: 0.892–0.977), with a Youden index of 0.811, sensitivity of 88.46%, and specificity of 92.59%. These results were superior compared to the diagnosis using each Mp-MRI parameter and the LI-RADS classification standard alone. A significant difference in the LI-RADS classification of nodules of different pathological grades was observed in the malignant group ($P < 0.05$). The ER, MET, MSI, and ADC were

基金项目:河南省医学科技攻关计划(联合共建)项目(LHGJ20210431)
作者简介:蔡宁(1991-),女,主治医师,硕士.
通信作者:蔡宁,E-mail:caining1478@126.com
收稿日期:2023-09-14
网络出版时间:2024-07-23 10:55:11

highest in well-differentiated nodules, followed by moderately differentiated nodules, and were lowest in poorly differentiated nodules. FF and MSD were highest in poorly differentiated nodules, followed by moderately differentiated nodules, and were lowest in well-differentiated nodules ($P < 0.05$). Spearman's correlation analysis showed that the LI-RADS classification and Mp-MRI parameters ER, MET, MSI, and ADC were positively correlated with the pathological grade of SHCC, whereas FF and MSD were negatively correlated with the pathological grade of SHCC ($P < 0.05$). **Conclusion** The combination of Mp-MRI parameters and the LI-RADS classification criteria is reliable for diagnosing regenerative nodules in cirrhosis and SHCC and can provide important reference information for the clinical evaluation of SHCC pathological grading.

Keywords regenerated nodules in cirrhosis; small hepatocellular carcinoma; multi-parameter magnetic resonance imaging; grading standards for liver imaging reporting and data management systems; diagnostic value

小肝癌（small hepatocellular carcinoma，SHCC）是临床常见的肝细胞癌类型，具有病灶体积小、生长缓慢等特点，5年生存率>50%，且部分患者可治愈[1-2]。尽早确诊并给予有效治疗是降低SHCC死亡率、提高治愈率及生存率的关键[3]。研究[4]证实，肝硬化再生结节是肝硬化进展至SHCC的重要阶段，需及时进行鉴别诊断。目前，临床诊断SHCC的“金标准”为细针穿刺或手术切除的标本病理活检。活检为有创操作，且具有获取标本量小、穿刺部位不准确、时间滞后等特点，不但影响诊断结果，甚至会延误最佳治疗时机[5]。肝脏影像报告和数据管理系统（liver imaging reporting and data system，LI-RADS）分级属于标准化肝脏病灶分级诊断系统，能准确判断肝脏病灶的危险性，但有研究[6-7]表明，单纯应用该分级标准诊断SHCC存在一定误差。多参数磁共振成像（multi-parameter magnetic resonance imaging，Mp-MRI）是一种新型MRI成像方式，能通过多种参数定量评估肿瘤性质[8]。目前，尚未有Mp-MRI联合LI-RADS分级标准鉴别诊断肝硬化再生结节与SHCC的报道，本研究围绕该课题展开探讨分析，以期为临床提供参考。

1　材料与方法

1.1　一般资料

选取2019年3月至2023年3月我院肝脏结节直径≤3 cm的患者86例（132个结节），根据手术病理结果将肝硬化再生结节38例（54个结节）记为良性组，SHCC 48例（78个结节）记为恶性组。本研究获得郑州大学第二附属医院伦理委员会批准。

1.2　选取标准

纳入标准：肝脏结节直径≤3 cm，均经病理检查证实结节性质，恶性组诊断均为SHCC，良性组诊断均为肝硬化再生结节；患者均知晓自身病情及研究方案，自愿签署知情同意书。排除标准：参与本研究前接受过抗肿瘤治疗；合并其他类型肝脏疾病；存在遗传性代谢性疾病；有酗酒史；存在MRI检查禁忌。

1.3　方法

1.3.1　MRI检查方法：采用Magnetom Skyra 3.0T MRI扫描仪（购自西门子公司）进行检查，检查前叮嘱患者禁食6~8 h，首先行常规平扫，包括冠状位T2WI扫描、横轴位T1WI、T2WI、扩散加权成像（DWI）扫描，b值选取800 s/mm^2、1 000 s/mm^2；再分别行冠状位、横轴位T1WI增强扫描，于肘静脉注射0.2 mL/kg造影剂（钆贝葡胺注射液），速率为2.5 mL/s，于造影剂注射15 s后行动脉期扫描，50 s后行门脉期扫描，120 s后行延迟期扫描。将所有图像数据传送至工作站进行图像处理，测量增强率（enhancement rate，ER）、平均强化时间（mean time to enhancement，MET）、最大上升斜率（maximum slope of increase，MSI）、最大下降斜率（maximum slope of decrease，MSD）、表观扩散系数（apparent diffusion coefficient，ADC）和脂肪分数（fat fraction，FF）。

1.3.2　LI-RADS分级标准：根据MRI检查结果判定LI-RADS分级，阴性包括LR-1级、LR-2级、LR-3级，阳性包括LR-4级、LR-5级[9]。

1.4　观察指标

对比2组一般资料；统计LI-RADS分级诊断结果；对比2组Mp-MRI参数，包括ER、MET、MSI、MSD、ADC、FF；分析Mp-MRI联合LI-RADS分级标准对肝硬化再生结节与SHCC的诊断价值；对比恶性组不同病理分级结节LI-RADS分级和Mp-MRI参数；分析LI-RADS分级、Mp-MRI参数与SHCC病理分级的相关

性。

1.5　统计学分析

采用EpiData 3.1建立数据库，采用SPSS 22.0统计软件进行统计分析。计量资料行Kolmogorov-Smirnov正态性检验和Levene法方差齐性检验，正态分布且方差齐性时以$\bar{x} \pm s$表示，2组比较采用t检验；计数资料以率（%）表示，2组比较采用χ^2检验；采用受试者操作特征（receiver operating characteristic，ROC）曲线及曲线下面积（area under the curve，AUC）分析诊断价值；采用Spearman相关分析相关性。$P < 0.05$为差异有统计学意义。

2　结果

2.1　2组一般资料比较

2组年龄、性别、结节直径等比较无统计学差异（$P > 0.05$），一般资料均衡可比。见表1。

表1　2组一般资料比较

Tab.1　Comparison of general information of the two groups

Group	Malignant group (n = 48)	Benign group (n = 38)	t/χ^2	P
Sex [n (%)]			0.045	0.831
Male	40 (83.33)	31 (81.58)		
Female	8 (16.67)	7 (18.42)		
Age (year)	55.92 ± 5.17	55.19 ± 5.63	0.625	0.534
Nodule diameter (cm)	1.60 ± 0.16	1.57 ± 0.18	0.817	0.416

2.2　LI-RADS分级诊断结果

经LI-RADS分级标准诊断，良性组检出LR-1级12个，LR-2级21个，LR-3级11个，LR-4级7个，LR-5级3个，恶性组检出LR-1级1个，LR-2级7个，LR-3级4个，LR-4级36个，LR-5级30个。2组132个结节中共检出阳性76个，阴性56个。其中，假阳性10个，假阴性12个。ROC曲线分析结果显示，LI-RADS分级标准诊断肝硬化再生结节与SHCC的AUC为0.827（95%*CI*：0.752~0.887），约登指数为0.654，灵敏度为86.84%，特异度为78.57%，见图1。

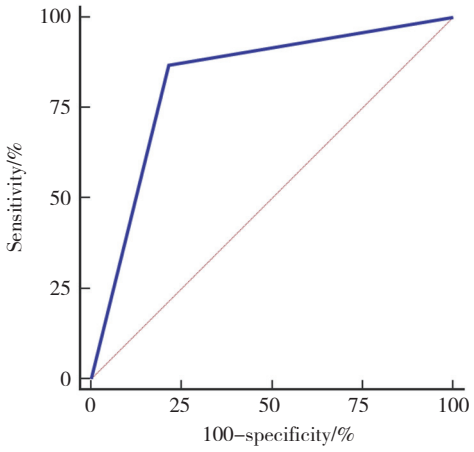

图1　LI-RADS分级标准诊断结果

Fig.1　Diagnostic results of the LI-RADS grading criteria

2.3　2组Mp-MRI参数及诊断结果

恶性组ER、MET、MSI、ADC低于良性组，FF、MSD高于良性组（$P < 0.05$），见表2。

表2　2组Mp-MRI参数比较（$\bar{x} \pm s$）

Tab.2　Comparison of the Mp-MRI parameters between the two groups ($\bar{x} \pm s$)

Group	n	ER (%)	MET (s)	MSI	MSD	ADC ($\times 10^{-3}$ mm^2/s)	FF (Hz)
Malignant group	78	67.68 ± 8.91	510.57 ± 16.20	108.41 ± 35.62	115.23 ± 28.79	0.98 ± 0.17	4.65 ± 1.48
Benign group	54	81.32 ± 10.64	533.28 ± 21.75	161.53 ± 47.19	89.60 ± 20.56	1.13 ± 0.22	2.51 ± 0.80
t		7.982	6.874	7.366	5.622	4.414	9.684
P		<0.001	<0.001	<0.001	<0.001	<0.001	<0.001

ER、MET、MSI、MSD、ADC、FF诊断肝硬化再生结节与SHCC的AUC分别为0.777（95%*CI*：0.696~0.844）、0.716（95%*CI*：0.631~0.791）、0.746（95%*CI*：0.663~0.818）、0.833（95%*CI*：0.758~0.892）、0.792（95%*CI*：

0.713~0.858)、0.764(95%*CI*:0.682~0.834),约登指数分别为0.489、0.412、0.422、0.593、0.477、0.547,灵敏度分别为85.90%、78.21%、71.79%、83.33%、88.46%、60.26%,特异度分别为62.96%、62.96%、70.37%、75.93%、59.26%、94.44%,见图2。

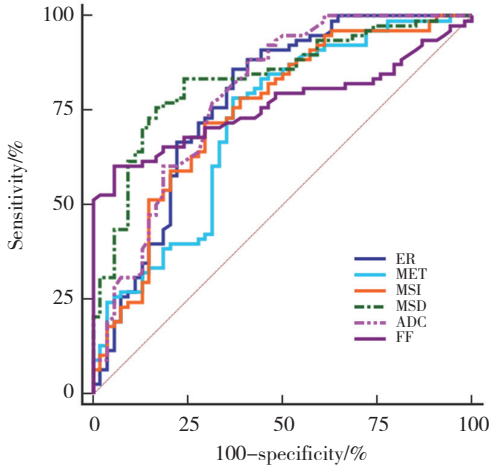

图2　Mp-MRI参数诊断结果

Fig.2　Results of the Mp-MRI parameter diagnosis

2.4　Mp-MRI联合LI-RADS分级标准对肝硬化与再生结节与SHCC的诊断价值

将Mp-MRI参数ER、MET、MSI、MSD、ADC、FF与LI-RADS分级进行logistic二元回归分析,返回预测概率Logit(*P*)作为独立检验变量,获取Mp-MRI参数联合LI-RADS分级标准诊断肝硬化再生结节与SHCC的AUC为0.946(95%*CI*:0.892~0.977),约登指数为0.811,灵敏度为88.46%,特异度为92.59%,优于各Mp-MRI参数及LI-RADS分级单独诊断,见图3。

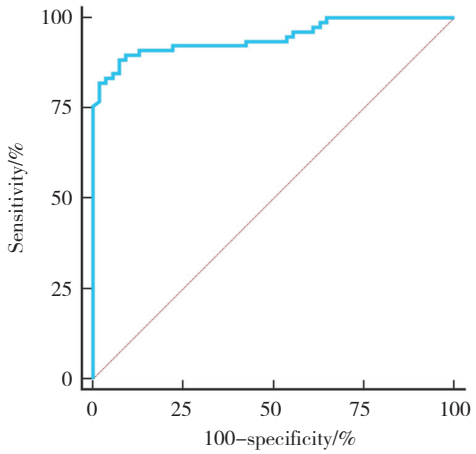

图3　Mp-MRI联合LI-RADS分级标准对肝硬化与再生结节与SHCC的诊断价值

Fig.3　Value of Mp-MRI combined with the LI-RADS grading criteria in the diagnosis of cirrhosis with regenerated nodules and SHCC

2.5　恶性组不同病理分级结节LI-RADS分级、Mp-MRI参数比较

恶性组不同病理分级结节LI-RADS分级比较,差异有统计学意义($U = 19.588$,$P < 0.001$),见表3。ER、MET、MSI、ADC在高分化结节中最高,中分化结节次之,低分化结节最低,FF、MSD在低分化结节最高,中分化结节次之,高分化结节最低($P < 0.05$),见表4。

表3　恶性组不同病理分级结节LI-RADS分级比较[*n* (%)]

Tab.3　Comparison of LI-RADS grades of nodules with different pathological grades in the malignant group [*n* (%)]

Group	*n*	Level LR-1	Level LR-2	Level LR-3	Level LR-4	Level LR-5
Poorly differentiated	24	0(0)	1(4.17)	0(0)	5(20.83)	18(75.00)
Moderately differentiated	33	0(0)	2(6.06)	1(3.03)	20(60.61)	10(30.30)
Highly differentiated	21	1(4.76)	4(19.05)	3(14.29)	11(52.38)	2(9.52)

表4　恶性组不同病理分级结节Mp-MRI参数比较($\bar{x} \pm s$)

Tab.4　Comparison of Mp-MRI parameters of nodules with different pathological grades in the malignant group ($\bar{x} \pm s$)

Group	*n*	ER(%)	MET(s)	MSI	MSD	ADC($\times 10^{-3}$ mm^2/s)	FF(Hz)
Poorly differentiated	24	60.21 ± 6.15	492.72 ± 10.59	88.68 ± 20.03	131.24 ± 19.66	0.84 ± 0.06	5.71 ± 1.26
Moderately differentiated	33	68.19 ± 6.93	514.46 ± 12.34	107.57 ± 22.41	112.29 ± 22.58	1.01 ± 0.09	4.58 ± 1.09
Highly differentiated	21	75.42 ± 7.22	524.86 ± 15.81	132.28 ± 26.89	101.55 ± 27.14	1.09 ± 0.10	3.55 ± 1.02
F		28.331	37.450	20.119	9.734	52.179	20.664
P		<0.001	<0.001	<0.001	<0.001	<0.001	<0.001

2.6　LI-RADS分级、Mp-MRI参数与SHCC病理分级的相关性

Spearman相关性分析结果显示，LI-RADS分级、Mp-MRI参数ER、MET、MSI、ADC与SHCC病理分级呈正相关，FF、MSD与SHCC病理分级呈负相关（$P<0.05$），见表5。

表5　LI-RADS分级、Mp-MRI参数与SHCC病理分级的相关性

Tab.5　Correlation between LI-RADS grading，Mp-MRI parameters，and SHCC pathological grading

Index	Pathological grade	
	r	*P*
LI-RADS classification	0.628	<0.001
ER	0.614	<0.001
MET	0.572	<0.001
MSI	0.649	<0.001
MSD	−0.553	<0.001
ADC	0.704	<0.001
FF	−0.693	<0.001

3　讨论

近年来随着造影剂的应用及MRI扫描序列增多，Mp-MRI逐渐应用于良恶性病变诊断中，可经多方式、多角度成像为临床早期筛查恶性病变提供依据[10]。王立鹏等[11]研究指出，Mp-MRI能显著提高前列腺癌检出率。相关研究[12]表明，SHCC组织结构与正常肝脏组织相比更为复杂，应用MRI检查时相关参数通常呈异常表达趋势，能有效反映结节性质。本研究结果显示，恶性组ER、MET、MSI、ADC低于良性组，FF、MSD高于良性组。分析原因，Mp-MRI除了能通过造影剂分布与清除情况判断结节大小、形态与范围，还能经由多参数呈现结节内部多方面的影像改变特征，其中MSI、MSD是反映结节病灶内部微循环血供速度、血流量的影像参数，MET提示造影剂通过结节组织的时间，FF反映结节内部脂肪水平，ER表示的是肝细胞表面受体表达水平，ADC是评估结节组织内水分子扩散情况的指标，SHCC组织内部存在新生血管丰富、血供多、血流速度快、脂肪沉积较多及细胞密度较高等特点，从而导致上述参数在肝硬化再生结节与SHCC中呈现出明显差异[13-14]。ROC曲线分析结果显示，ER、MET、MSI、MSD、ADC、FF诊断肝硬化再生结节与SHCC的AUC均>0.7，提示Mp-MRI参数能作为临床鉴别诊断肝硬化再生结节与SHCC的影像学指标。

SHCC虽然具有典型影像学表现，但非标准化影像学报告存在描述不准确、表达不清晰等局限性[15-16]。LI-RADS分级标准是将肝癌超声、CT、MRI影像学报告进行标准化描述的分级系统，具有更易理解、描述更准确、表达更清晰的优势[17]。本研究结果显示，LI-RADS分级标准诊断SHCC的灵敏度为86.84%，特异度为78.57%，提示其具有较好的诊断价值。LI-RADS分级标准综合了结节大小、形态、生长速度、包膜、强化方式等多种因素，对结节癌变的可能性进行分级诊断，能尽可能减少不典型SHCC影像表现被漏诊的情况[18]。但LI-RADS分级标准中多考虑定性影像学表现，忽略了定量参数在临床诊断中的作用。本研究发现，Mp-MRI参数联合LI-RADS分级标准诊断的AUC高达0.946，优于各Mp-MRI参数及LI-RADS分级单独诊断，提示临床可将Mp-MRI参数联合LI-RADS分级标准作为早期SHCC的优选诊断方式。

此外，本研究还观察到LI-RADS分级、Mp-MRI参数ER、MET、MSI、ADC与SHCC病理分级呈正相关，FF、MSD与SHCC病理分级呈负相关，可见Mp-MRI参数与LI-RADS分级标准能为临床准确评估SHCC病理分级提供参考依据。但本研究未详细探讨Mp-MRI参数联合LI-RADS分级标准对SHCC病理分级的具体评估价值，后续仍需进一步探讨。

综上所述，Mp-MRI参数联合LI-RADS分级标准诊断肝硬化再生结节与SHCC的价值可靠，且能为临床评估SHCC病理分级提供辅助诊断信息，但其临床意义仍需要进一步的深入研究。

参考文献：

[1] KAMAL MA，MANDOUR YM，ABD EL-AZIZ MK，et al. Small molecule inhibitors for hepatocellular carcinoma：advances and challenges [J]. Molecules，2022，27（17）：5537. DOI：10.3390/molecules27175537.

[2] 杨帆，曹毛毛，李贺，等. 1990–2019年中国人群肝癌流行病学趋势分析及预测 [J]. 中华消化外科杂志，2022，21（1）：106-113. DOI：10.3760/cma.j.cn115610-20211203-00616.

[3] SEAGER MJ. Radiation segmentectomy for small，solitary hepatocellular carcinoma [J]. Radiol Imaging Cancer，2021，3（2）：e219006. DOI：10.1148/rycan.2021219006.

[4] DUAN Y，XIE XY，LI Q，et al. Differentiation of regenerative nodule，dysplastic nodule，and small hepatocellular carcinoma in cirrhotic patients：a contrast-enhanced ultrasound-based multivariable model analysis [J]. Eur Radiol，2020，30（9）：4741-4751. DOI：10.1007/s00330-020-06834-5.

[5] YAMADA A. Editorial for “preoperative evaluation of Gd-EOB-DT-

PA-enhanced MRI radiomics-based nomogram in small solitary hepatocellular carcinoma (≤3 cm) with microvascular invasion: a two-center study" [J]. J Magn Reson Imaging, 2022, 56 (5): 1473-1474. DOI: 10.1002/jmri.28188.
[6] 王影, 余深平. LI-RADS与亚洲肿瘤峰会标准对小肝癌的诊断效能分析[J]. 中山大学学报(医学版), 2019, 40 (3): 473-480. DOI: 10.13471/j.cnki.j.sun.yat-sen.univ (med.sci).2019.0067.
[7] VAN DER POL CB, MCINNES MDF, SALAMEH JP, et al. CT/MRI and CEUS LI-RADS major features association with hepatocellular carcinoma: individual patient data meta-analysis [J]. Radiology, 2022, 302 (2): 326-335. DOI: 10.1148/radiol.2021211244.
[8] KAO S, SUNG K. Editorial for "predicting the outcome of transcatheter arterial embolization therapy for unresectable hepatocellular carcinoma based on radiomics of preoperative multiparameter MRI" [J]. J Magn Reson Imaging, 2020, 52 (4): 1091-1092. DOI: 10.1002/jmri.27166.
[9] 张大福, 李振辉, 段学昆, 等. LI-RADS MRI分类标准对肝细胞癌的诊断效能[J]. 放射学实践, 2016, 31 (4): 303-306. DOI: 10.13609/j.cnki.1000-0313.2016.04.005.
[10] 白晶晶, 张璐, 王效春, 等. 基于多参数磁共振成像的影像组学在膀胱癌精准诊疗中的研究进展[J]. 磁共振成像, 2022, 13 (11): 157-160. DOI: 10.12015/issn.1674-8034.2022.11.032.
[11] 王立鹏, 阳青松, 张威, 等. 多参数磁共振成像在前列腺癌中的诊断价值[J]. 第二军医大学学报, 2019, 40 (11): 1236-1241. DOI: 10.16781/j.0258-879x.2019.11.1236.
[12] SUGAWARA Y, HIBI T. Surgical treatment of hepatocellular carcinoma [J]. Biosci Trends, 2021, 15 (3): 138-141. DOI: 10.5582/bst.2021.01094.
[13] LUO JP, HUANG ZM, WANG MR, et al. Prognostic role of multiparameter MRI and radiomics in progression of advanced unresectable hepatocellular carcinoma following combined transcatheter arterial chemoembolization and lenvatinib therapy [J]. BMC Gastroenterol, 2022, 22 (1): 108. DOI: 10.1186/s12876-022-02129-9.
[14] 唐玉峰, 臧晨, 苗园园. 磁共振多参数定量技术在诊断肝癌结节中的临床应用[J]. 实用癌症杂志, 2022, 37 (10): 1674-1677. DOI: 10.3969/j.issn.1001-5930.2022.10.029.
[15] KIM TH, WOO S, JOO I, et al. LI-RADS treatment response algorithm for detecting incomplete necrosis in hepatocellular carcinoma after locoregional treatment: a systematic review and meta-analysis using individual patient data [J]. Abdom Radiol (NY), 2021, 46 (8): 3717-3728. DOI: 10.1007/s00261-021-03122-8.
[16] CHOI SJ, CHOI SH, KIM DW, et al. Value of threshold growth as a major diagnostic feature of hepatocellular carcinoma in LI-RADS [J]. J Hepatol, 2023, 78 (3): 596-603. DOI: 10.1016/j.jhep.2022.11.006.
[17] 刘晓宇, 缪建良, 应世红, 等. 比较亚洲肿瘤峰会标准与LI-RADS对乙型肝炎性小肝癌的诊断价值[J]. 中国介入影像与治疗学, 2020, 17 (11): 671-674. DOI: 10.13929/j.issn.1672-8475.2020.11.008.
[18] ZHONG X, TANG HS, GUAN TP, et al. Added value of quantitative apparent diffusion coefficients for identifying small hepatocellular carcinoma from benign nodule categorized as LI-RADS 3 and 4 in cirrhosis [J]. J Clin Transl Hepatol, 2022, 10 (1): 34-41. DOI: 10.14218/JCTH.2021.00053.

(编辑　于　溪)

(上接第685页)

2017, 60 (1): 58-81. DOI: 10.1097/GRF.0000000000000264.
[4] 夏志军. 女性泌尿盆底疾病临床诊治[M]. 北京: 人民卫生出版社, 2016: 377-379.
[5] HILDE G, STÆR-JENSEN J, SIAFARIKAS F, et al. Impact of childbirth and mode of delivery on vaginal resting pressure and on pelvic floor muscle strength and endurance [J]. Am J Obstet Gynecol, 2013, 208 (1): 50.e1-50.e7. DOI: 10.1016/j.ajog.2012.10.878.
[6] SIAHKAL SF, IRAVANI M, MOHAGHEGH Z, et al. Investigating the association of the dimensions of genital hiatus and levator hiatus with pelvic organ prolapse: a systematic review [J]. Int Urogynecol J, 2021, 32 (8): 2095-2109. DOI: 10.1007/s00192-020-04639-0.
[7] HOROSZ E, POMIAN A, ZWIERZCHOWSKA A, et al. Epidemiological features of the bladder neck rest position and mobility [J]. J Clin Med, 2020, 9 (8): 2413. DOI: 10.3390/jcm9082413.
[8] 张国慧, 岳嵩, 玄英华, 等. 子宫位置与盆腔器官脱垂的关系[J]. 中国超声医学杂志, 2024, 40 (3): 320-323. DOI: 10.3969/j.issn.1002-0101.2024.03.025.
[9] DELANCEY JOL, MASTELING M, PIPITONE F, et al. Pelvic floor injury during vaginal birth is life-altering and preventable: what can we do about it? [J]. Am J Obstet Gynecol, 2024, 230 (3): 279-294.e2. DOI: 10.1016/j.ajog.2023.11.1253.
[10] RUSAVY Z, PAYMOVA L, KOZEROVSKY M, et al. Levator ani avulsion: a systematic evidence review (LASER) [J]. BJOG, 2022, 129 (4): 517-528. DOI: 10.1111/1471-0528.16837.
[11] 陶均佳, 应涛, 陈爱萍, 等. 断层超声成像技术在分娩时耻骨直肠肌损伤诊断中的应用[J]. 中国医科大学学报, 2023, 52 (2): 179-182. DOI: 10.12007/j.issn.0258-4646.2023.02.016.
[12] VAN DELFT KWM, THAKAR R, SULTAN AH, et al. The natural history of levator avulsion one year following childbirth: a prospective study [J]. BJOG, 2015, 122 (9): 1266-1273. DOI: 10.1111/1471-0528.13223.
[13] HANDA VL, ROEM J, BLOMQUIST JL, et al. Pelvic organ prolapse as a function of levator ani avulsion, hiatus size, and strength [J]. Am J Obstet Gynecol, 2019, 221 (1): 41.e1-41.e7. DOI: 10.1016/j.ajog.2019.03.004.
[14] VAN DE WAARSENBURG MK, VERBERNE EA, VAN DER VAART CH, et al. Recovery of puborectalis muscle after vaginal delivery: an ultrasound study [J]. Ultrasound Obstet Gynecol, 2018, 52 (3): 390-395. DOI: 10.1002/uog.18976.
[15] CHENG WJ, ENGLISH E, HORNER W, et al. Hiatal failure: effects of pregnancy, delivery, and pelvic floor disorders on level Ⅲ factors [J]. Int Urogynecol J, 2023, 34 (2): 327-343. DOI: 10.1007/s00192-022-05354-8.
[16] BARCA JA, BRAVO C, PINTADO-RECARTE MP, et al. Pelvic floor morbidity following vaginal delivery versus cesarean delivery: systematic review and meta-analysis [J]. J Clin Med, 2021, 10 (8): 1652. DOI: 10.3390/jcm10081652.
[17] BLOMQUIST JL, CARROLL M, MUÑOZ A, et al. Pelvic floor muscle strength and the incidence of pelvic floor disorders after vaginal and cesarean delivery [J]. Am J Obstet Gynecol, 2020, 222 (1): 62.e1-62.e8. DOI: 10.1016/j.ajog.2019.08.003.
[18] BARBOSA AMP, MARINI G, PICULO F, et al. Prevalence of urinary incontinence and pelvic floor muscle dysfunction in primiparae two years after cesarean section: cross-sectional study [J]. Sao Paulo Med J, 2013, 131 (2): 95-99. DOI: 10.1590/s1516-31802013000100019.

(编辑　陈　姜)